The $(d, {}^2\mathrm{He})$ reaction on ^{76}Se and the double-β-decay matrix elements for $A = 76$

E.-W. Grewe,[1] C. Bäumer,[1,*] H. Dohmann,[1] D. Frekers,[1] M. N. Harakeh,[2] S. Hollstein,[1] H. Johansson,[3,†] L. Popescu,[4,‡] S. Rakers,[1,§] D. Savran,[2,5] H. Simon,[3] J. H. Thies,[1] A. M. van den Berg,[2] H. J. Wörtche,[2] and A. Zilges[6]

[1]*Institut für Kernphysik, Westfälische Wilhelms-Universität, D-48149 Münster, Germany*

[2]*Kernfysisch Versneller Instituut, University of Groningen, NL-9747 AA Groningen, The Netherlands*

[3]*Gesellschaft für Schwerionenforschung, D-63291 Darmstadt, Germany*

[4]*Vakgroep Subatomaire en Stralingsfysica, Universiteit Gent, B-9000 Gent, Belgium*

[5]*Institut für Kernphysik, Technische Universität Darmstadt, D-64289 Darmstadt, Germany*

[6]*Institut für Kernphysik, Universität zu Köln, D-50937 Köln, Germany*

(Received 21 January 2008; published 8 October 2008)

The $(d, {}^2\mathrm{He})$ charge-exchange reaction on ^{76}Se was studied at an incident energy of 183 MeV. The outgoing two protons in the $^1S_0$ state, referred to as ^{2}He, were both momentum analyzed and detected by the same spectrometer and detector. The experiment was performed at KVI, Groningen, using the magnetic spectrometer BBS at three angular positions: 0°, 2.5°, and 5°. Excitation-energy spectra of the residual nucleus ^{76}As were obtained with an energy resolution of about 120 keV (FWHM). Gamow-Teller (GT^+) transition strengths were extracted up to 5 MeV and compared with those from an (n, p) experiment at low resolution. Together with the GT^- transition strengths from the $^{76}\mathrm{Ge}(p, n)$ experiment leading to the same intermediate nucleus, the nuclear matrix element of the two-neutrino double-β decay of ^{76}Ge was evaluated.

DOI: 10.1103/PhysRevC.78.044301 PACS number(s): 25.45.Kk, 21.10.−k, 23.40.Hc, 27.50.+e

I. INTRODUCTION

Charge-exchange reactions of (p, n) and (n, p) type at intermediate energies and at low momentum transfers ($q_{\mathrm{tr}} \sim 0$) feature a high selectivity for Gamow-Teller (GT) transitions. The selectivity is a direct consequence of the strong $V_{\sigma\tau}$ component of the effective interaction [1–4] in this particular kinematic window. Because the same $\sigma\tau$ operator is active in the weak process of nuclear β decay, the GT^+ and GT^- transition strengths extracted from the (n, p)- and (p, n)-type charge-exchange reactions can therefore also be used to construct the two "legs" of the two-neutrino double-β ($2\nu\beta\beta$)-decay matrix element, thereby providing an important input to nuclear models aimed at describing foremost the 2ν and, to a lesser extent, the $0\nu\beta\beta$ decay. The virtues of charge-exchange reactions and, in particular, those of the high resolution that can be obtained via the $(d, {}^2\mathrm{He})$ and the $({}^3\mathrm{He}, t)$ reactions have recently been demonstrated for the $\beta\beta$-decay nuclei ^{48}Ca, ^{64}Zn, and ^{116}Cd [5–7].

The present article focuses on the GT transition to ^{76}As via the $^{76}\mathrm{Se}(d, {}^2\mathrm{He})^{76}\mathrm{As}$ reaction. ^{76}Se is the final nucleus in the $\beta\beta$ decay of ^{76}Ge, for which the two-neutrino decay has been observed and for which the neutrinoless mode is presently the subject of two large-scale counting experiments, GERDA [8] and Majorana [9].

The decay scheme of ^{76}Ge is sketched in Fig. 1. One may note that the ground state of ^{76}As has a spin-parity of $J^\pi = 2^-$, and therefore the 2ν decay path of the $\beta\beta$ decay only involves excited states in ^{76}As, unlike the $0\nu\beta\beta$ decay, for which the ground-state path may be quite relevant [10,11]. Of course, the 0ν decay involves a multitude of levels of many multipolarities up to considerable momentum transfers ($q \sim 0.5\ \mathrm{fm}^{-1}$), of which those that are mediated by the GT operator of the 2ν decay are only a small subset. Certainly, charge-exchange reactions cannot completely unravel them.

The $2\nu\beta\beta$-decay half-life of ^{76}Ge has been determined by several counting experiments. In Refs. [13–16] half-life values have been reported, which are all close to $T_{1/2}^{(2\nu)} \approx 1 \times 10^{21}$ yr. The Heidelberg-Moscow group, on the other hand, reported a value of about $T_{1/2}^{(2\nu)} \approx 1.7 \times 10^{21}$ yr [17–20]. This has led to an average value of $T_{1/2}^{(2\nu)} = (1.5 \pm 0.1) \times 10^{21}$ yr recently recommended by Barabash [21].

From the theory side, the ^{76}Ge $\beta\beta$ decay has been the subject of numerous calculations, using either the shell model as the underlying basis or various types of the quasiparticle random-phase-approximation (QRPA). By and large, the models also seem to converge to a value of 1.5×10^{21} yr [22–29], with a few marked exceptions showing deviations as large as an order of magnitude [30–32]. We do not want to enter into a debate of the various differences, except that the issue of the nuclear matrix elements always seems to be at the center of the discussion [10,11,33–35].

Early experiments to measure the $2\nu\beta\beta$-decay matrix elements from which to evaluate the $2\nu\beta\beta$-decay half-life have been presented in Refs. [36,37]. Here, the relevant (p, n) measurements were performed at the IUCF SWINGER facility [37,38] and the (n, p) measurements at the TRIUMF CHARGEX setup [36,39]. Unfortunately, in all of these measurements the energy resolution was a rather limiting

*Present address: PHILIPS Research Europe, 52066 Aachen, Germany.

†Present address: Fundamental Fysik, Chalmers Tekniska Högskola, S-412 96, Göteborg, Sweden.

‡Present address: NIPNE, Bucharest, Romania.

§Present address: EADS Astrium Space Transportation GmbH, TE53 Avionics Engineering, 28199 Bremen, Germany.

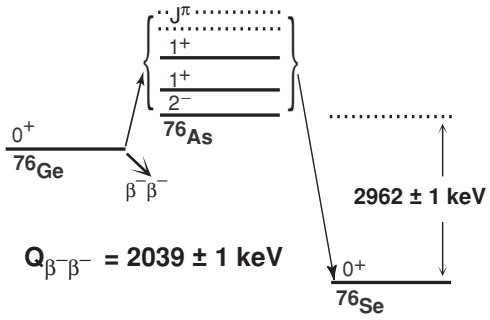

FIG. 1. Schematic representation of the $\beta\beta$ decay of ^{76}Ge [12]. Whereas in the $2\nu\beta\beta$ mode only the intermediate 1^+ states are relevant, there is a multitude of J^π states involved in the neutrinoless mode.

factor, which in the case of the (n, p) experiments was about 1.8 MeV and in the (p, n) experiments of order 350 keV.

In this article, we present results from a (n, p)-type ^{76}Se$(d, ^2$He$)^{76}$As charge-exchange experiment, which was performed at an incident deuteron energy of 183 MeV with 120 keV resolution. The high-resolution GT$^+$ strength distribution extracted from this experiment is then compared with the early (n, p) measurement performed by Helmer *et al.* [36]. To further construct the $2\nu\beta\beta$-decay matrix element, the GT$^-$ distribution deduced from the (p, n) experiment on ^{76}Ge by Madey *et al.* [37] is employed, by which the half-life for the ^{76}Ge $2\nu\beta\beta$ decay can be evaluated.

II. EXPERIMENT

The $(d, ^2$He) experiment was performed at the AGOR facility of the KVI, Groningen [40,41], where the deuterons were accelerated up to 183 MeV. Outgoing two protons in a $^1S_0$ state denoted as ^{2}He were both momentum analyzed in the Big-Bite magnetic spectrometer (BBS) and detected in coincidence by the EUROSUPERNOVA detector (ESN detector) [41–43].

Beam line and BBS were set up in dispersion-matched mode for optimum energy resolution. Beam currents were measured by a Faraday cup inside the spectrometer and ranged between 0.4 and 1.5 nA. The BBS was set to $\Theta_{\rm BBS} = 0^\circ$, 2.5°, and 5° to obtain angular distributions. The ESN detector consisted of a focal-plane detection system (FPDS) with two vertical-drift chambers (VDCs) located near the focal plane of the BBS. The standard setup for particle tracking consists of an additional set of four multiwire proportional chambers (MWPCs) [44]. The tracking is part of the trigger decision in order to suppress the contribution from the overwhelming deuteron breakup. It ensures a rather clean ^{2}He two-proton sample in the final data set. The target consisted of enriched ^{76}Se (99.7%) with a thickness of 2.3 ± 0.2 mg/cm^2. The material was sandwiched between two carbon foils of 0.2 mg/cm^2 thickness. A final-state energy resolution of about $\Delta E = 120$ keV was achieved.

Data acquisition and data analysis proceeded in the way as described in Refs. [5,7,45–53].

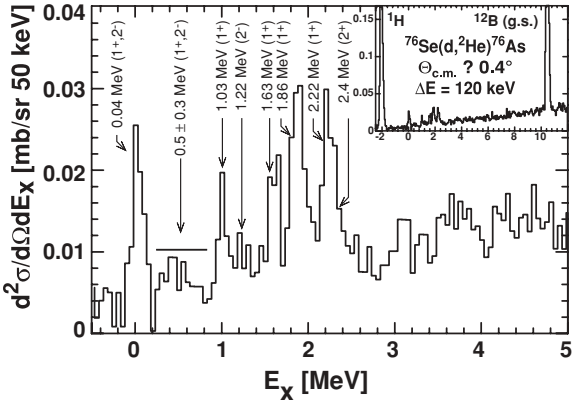

FIG. 2. Excitation-energy spectrum from the reaction ^{76}Se$(d, ^2$He$)^{76}$As. The spectrum was taken at a spectrometer angle of 0° and covers an angular range in the center-of-mass system between 0° and 1.3°. The J^π values of individual levels (or of a conglomerate of levels) were determined by the shape of the angular distributions. In the inset, the spectrum is shown for a wider excitation-energy range to show the dominating peaks resulting from the reactions ^{1}H$(d, ^2$He$)n$ and ^{12}C$(d, ^2$He$)^{12}$B(g.s.).

III. ANALYSIS

The $\Theta_{\rm BBS} = 0^\circ$ excitation-energy spectrum of the ^{76}Se$(d, ^2$He$)(^{76}$As) reaction is shown in Fig. 2. The ground-state (g.s.) transition from ^{12}C, as well as the signal from the hydrogen contamination, which is frequently present in metal targets, were used for energy calibration. The ^{1}H$(d, ^2$He$)n$ transition appears in the 0° spectrum at $E_x \approx -2.2$ MeV in the excitation frame of ^{76}As. The associated peak quickly moves to higher excitation energies with increasing scattering angle and broadens. Therefore, the yield extraction for certain transitions and for certain scattering angles was not always possible, causing occasional gaps in the angular distributions.

A. DWBA analysis

To identify the J^π values of individual states, calculations of angular distributions were performed with the ACCBA code of Okamura [54] in distored-wave Born approximation (DWBA). The ACCBA code treats the $(d, ^2$He) reaction in an ordinary DW formalism and the three-body problem in the exit channel in an adiabatic approximation.

Further, an optical model is needed to describe the deuteron and proton wave functions in the entrance and exit channels. The deuteron optical-model parameters (OMPs) for the entrance channel were interpolated from global parameters derived for various nuclei up to $A = 116$ by Korff *et al.* [55], while proton OMPs were taken from Ref. [56]. It may be worth noting that the extraction of the B(GT) values does not depend on the OMPs to within reasonable bounds. The effective interaction was interpolated from the free NN t-matrix parametrizations of Franey and Love [57] to fit the projectile energy of 90 MeV/nucleon. The shell-model code NORMOD [58,59] was used to generate nuclear wave functions and one-body transition densities (OBTDs) assuming occupation

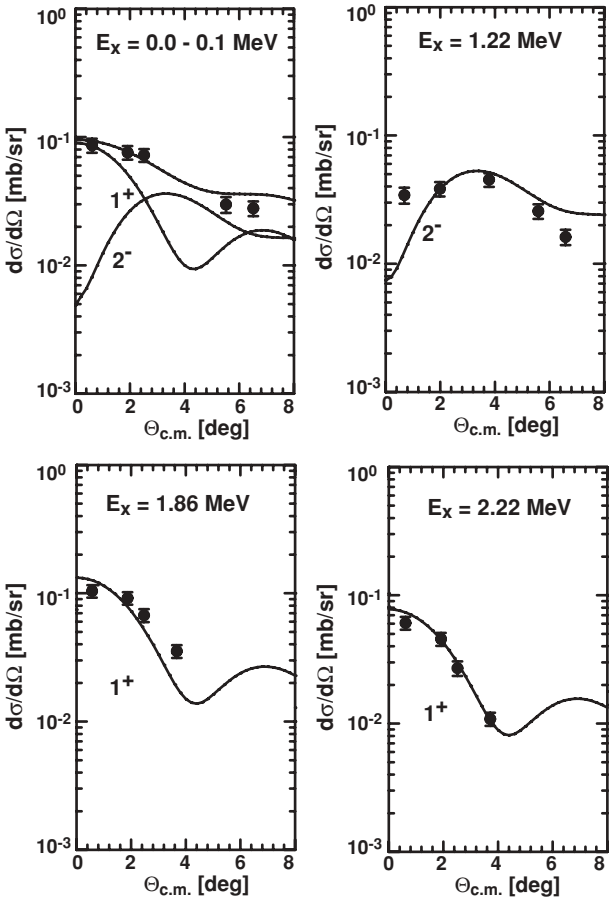

FIG. 3. Angular distributions of the levels excited in ^{76}As sorted by excitation energy. DWBA calculations are represented by solid lines. The error bars reflect the statistical errors and an additional 10% systematic error.

numbers deduced from a shell model with a smeared Fermi surface.

In the case of overlapping states a multipole-decomposition analysis was performed. This analysis was restricted to 1^+ and 2^- transitions only, as it was found that any higher multipoles did not significantly contribute to the cross section near zero degree. Angular distributions for $J^\pi = 1^+$ transitions can then easily be distinguished from those with $J^\pi = 2^-$, as the cross section rapidly decreases with increasing angle, which is opposite to the behavior of a $J^\pi = 2^-$ transition (cf. Fig. 3). Contributions from $\Delta L = 2$ to the 1^+ transitions are also possible, as these are mediated by the tensor-τ component of the effective interaction. However, this component is rather weak near zero momentum transfer [57]. Usually, such contributions are estimated to account for an extra systematic error for comparatively weakly excited transitions only [60–63]. Of course, tensor contributions are not connected to the ordinary β decay.

The excitation-energy spectrum of the ^{76}Se(d, ^{2}He)^{76}As reaction presented in Fig. 2 shows that a substantial fraction of the total GT strength seems to be shared among five strong transitions below 3 MeV. Above 3 MeV no isolated levels could be identified.

For all transitions indicated in Fig. 2 angular distributions were extracted and analyzed according to the above prescription. Examples are shown in Fig. 3, where we present the results for some well isolated levels. In some cases the procedure was also applied to wider energy bins, especially when nearby levels of different spins could not be resolved. For instance, the ground state of ^{76}As has a spin-parity $J^\pi = 2^-$, whereas the first excited $J^\pi = 1^+$ state lies at 0.044 MeV and two further $J^\pi = 1^+$ states are known at 0.086 and 0.128 MeV. Clearly, the present resolution is insufficient to resolve these levels, and we have therefore performed a combined analysis as is shown in the upper left part of Fig. 3. Judging from the peak shape in the 0° spectrum, we assume that most of the GT strength in the 0–0.1 MeV energy bin resides in the lower states at 0.044 and/or 0.086 MeV. The energies of the various other states and their spin-parity assignments are shown in Fig. 2. Note that the 1^+ level at 2.22 MeV has a close-by level. The level could not be analyzed at every angular setting, but the angular distribution features a flat characteristic, indicating a $\Delta L \neq 0$ transition.

To assess possible contributions from weakly excited GT transitions at the level of the detection limit, we performed a multipole decomposition of the angular distributions of two wide excitation-energy bins, one ranging from 0 to 5 MeV and the other from 5 to 10 MeV. These were described by a sum of 1^+, 2^-, and 3^+ transitions, though the analysis showed again that contributions from 3^+ transitions were not significant. The GT strength in the first bin from 0 to 5 MeV was evaluated to be $B\,(\mathrm{GT}) = 0.7 \pm 0.2$, which is slightly higher than the summed individual strengths of $\sum_{0-4\,\mathrm{MeV}} B\,(\mathrm{GT}) = 0.54 \pm 0.1$ given in Table I. In the second energy bin from 5 to 10 MeV, where in the zero degree spectrum no individual levels appear above the

TABLE I. Experimental cross sections at $q_{\mathrm{tr}} = 0$ and extracted $B(\mathrm{GT}^+)$ values. The errors in column 2 are evaluated from the counting rate and from a 10% uncertainty arising form the procedure of cross section extraction from angular distributions, both added in quadrature. The percentage of the non-GT cross sections at $q_{\mathrm{tr}} = 0$, which we identify as 2^- contributions from the multipole decomposition, is quoted in column 3. In column 4 we took the approach of ascribing 50% of this non-GT contribution to an additional uncertainty of the GT strength (added in quadrature). The results from the multipole decomposition of the energy bins (0–5 MeV) and (5–10 MeV) are quoted in the lower section of the table. Statistical and systematic uncertainties are indicated where appropriate.

E_x (MeV)	$d\sigma(q_{\mathrm{tr}} = 0)/d\Omega$ (mb/sr)	non-GT (2^-)	$B(\mathrm{GT}^+)$
0.04/0.08	0.087 ± 0.011	6%	0.102 ± 0.013
0.5±0.3	0.062 ± 0.008	14%	0.066 ± 0.012
1.03	0.070 ± 0.009	12%	0.076 ± 0.011
1.63	0.071 ± 0.009	13%	0.077 ± 0.011
1.86	0.114 ± 0.013	–	0.141 ± 0.016
2.22	0.063 ± 0.007	–	0.078 ± 0.009
Σ	$0.467\ ^{\pm 0.024(\mathrm{stat})}_{\pm 0.05(\mathrm{sys})}$		$0.54\ ^{\pm 0.03(\mathrm{stat})}_{\pm 0.08(\mathrm{sys})}$
0–5 MeV	$0.73 \pm 0.18(sys)$	15%	0.7 ± 0.2
5–10 MeV	$0.35 \pm 0.19(sys)$	22%	0.3 ± 0.2

detections limit of $B\,(\mathrm{GT}) = 0.05$, the summed GT strength was about 0.3 ± 0.2 units. Some caution may be in order, because for weakly excited states the tensor contributions may not be negligible [60–63]. These could reduce the above given values by a fair fraction.

B. Determination of Gamow-Teller strength

The GT strength was determined from the measured cross sections $\sigma_{\mathrm{exp}}(\Theta, q_{\mathrm{tr}})$ extrapolated to zero momentum transfer (i.e., $q_{\mathrm{tr}} = 0$) according to

$$\frac{d\sigma(q_{\mathrm{tr}}=0)}{d\Omega} = \frac{\sigma_{\mathrm{DWBA}}(q_{\mathrm{tr}}=0)}{\sigma_{\mathrm{DWBA}}(\Theta, q_{\mathrm{tr}})} \times \frac{d\sigma_{\mathrm{exp}}(\Theta, q_{\mathrm{tr}})}{d\Omega}, \qquad (1)$$

with the zero-momentum transfer cross section related to the $B(\mathrm{GT}^+)$ value via [3]

$$\frac{d\sigma(q_{\mathrm{tr}}=0)}{d\Omega} = C \cdot \left(\frac{\mu}{\pi\hbar^2}\right)^2 \frac{k_f}{k_i} N_D J_{\sigma\tau}^2 B(\mathrm{GT}^+). \qquad (2)$$

The parameter C is special to the $(d, {}^2\mathrm{He})$ reaction, as the cross section depends on the range of integration over the ^{2}He internal energy ε, and further includes possible effects of the more complicated nature of the $(d, {}^2\mathrm{He})$ reaction mechanism. It has been introduced as a constant scaling factor in nearly all $(d, {}^2\mathrm{He})$ analyses so far with a mean value of $C = 0.320 \pm 0.027$ [45–49], which was recently reconfirmed independently for the case of ^{64}Zn [7].

The distortion factor N_D in Eq. (2) is obtained from the ratio of the distorted-wave (DW) to plane-wave (PW) cross sections (see Ref. [47]):

$$N_D = \frac{\sigma_{\mathrm{DW}}(q_{\mathrm{tr}}=0)}{\sigma_{\mathrm{PW}}(q_{\mathrm{tr}}=0)}, \qquad (3)$$

which is $N_D = 0.042$ for the $^{76}\mathrm{Se}(d, {}^2\mathrm{He})^{76}\mathrm{As}$ reaction. The volume integral of the effective central $V_{\sigma\tau}$ interaction is taken as $|J_{\sigma\tau}| = 165$ MeV fm^3 [64].

The GT^+ strength values extracted according to this prescription are given in Table I.

C. Comparison with the ^{76}Se(n, p) reaction

Despite the much better resolution of the $(d, {}^2\mathrm{He})$ measurements, it may be instructive to compare the nuclear response of this reaction to the elementary $^{76}\mathrm{Se}(n, p)^{76}\mathrm{As}$ reaction, which was performed at TRIUMF with an energy resolution of 1.8 MeV [36]. To extract the $\Delta L = 0$, GT contribution from the (n, p) cross section two different methods were presented by the authors: the multipole decomposition of the total spectral response and the 6°-subtraction method. In the first case, angular distributions of 1 MeV energy bins up to 15° were described by a sum of calculated $\Delta L = 0$, 1, 2, and 3 transitions. The resulting $\Delta L = 0$ components were then transformed into $B(\mathrm{GT})$ values from which a summed value $\Sigma B\,(\mathrm{GT}) = 0.86 \pm 0.03$ for excitations up to 6 MeV was obtained. In the 6°-subtraction method one takes advantage of the fact that the $\Delta L = 0$ cross section decreases rapidly up to 6°, while the $\Delta L = 1$ cross section remains nearly constant. The $\Delta L = 1$ contribution at 6° was then subtracted from the total 0° cross section. The summed GT strength up to 6 MeV resulting from this method was $B(\mathrm{GT}) = 0.35 \pm 0.06$. It was noted, though, that this method has the tendency to estimate GT values, which are consistently smaller than those of the previous one [36,66].

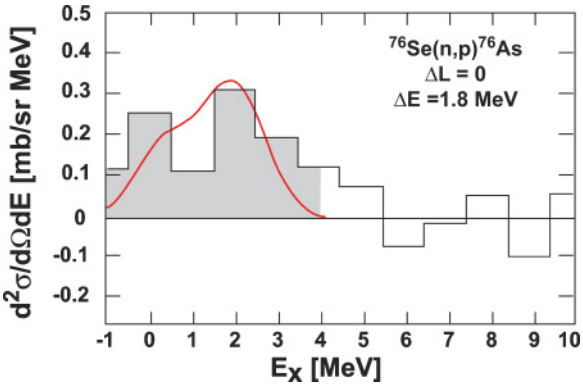

FIG. 4. (Color online) The $\Delta L = 0$, GT contribution to the $^{76}\mathrm{Se}(n, p)$ cross section deduced from (n, p) data using the 6°-subtraction method (histogram). The GT strength distribution from the present $(d, {}^2\mathrm{He})$ analysis was folded with a 1.8 MeV energy resolution to compare with the (n, p) analysis. The $(d, {}^2\mathrm{He})$ data were scaled to match the summed GT^+ strength included in the shaded area of the (n, p) data (refer to Table II). The (n, p) data were taken from Ref. [36].

The extracted $\Delta L = 0$ spectral component evaluated from the 6°-subtraction method is shown in Fig. 4. The full curve represents the GT^+ strength distribution deduced from the $(d, {}^2\mathrm{He})$ reaction on ^{76}Se folded with a 1.8 MeV resolution function to match the resolution of the (n, p) data. For this comparison, the GT strength, i.e., the $\Delta L = 0$ component from the $^{76}\mathrm{Se}(d, {}^2\mathrm{He})$ cross section was appropriately scaled using the values from Table II. The comparison gives credibility to

TABLE II. Comparison of the summed $B(\mathrm{GT}^+)$ strength deduced from the $(d, {}^2\mathrm{He})$ and (n, p) reactions on ^{76}Se. For the two methods of extracting GT strength from the (n, p) cross section one may refer to the text or Ref. [36]. Further, the experimental data are compared to a QRPA calculation by Engel *et al.* [65] with different values for g_{pp}. The theoretical summed GT strength includes levels up to $E_x \leqslant 10$ MeV.

	Method of analysis	$\Sigma B(\mathrm{GT}^+)$
$(d, {}^2\mathrm{He})$	Individual level cross sections	0.54 ± 0.11
$(d, {}^2\mathrm{He})$	(0–5 MeV) Integrated cross section	0.7 ± 0.2
(n, p)	6°-subtraction	0.35 ± 0.06
(n, p)	Multipole decomposition	0.86 ± 0.03
QRPA	g_{pp} (min)[a] = 130	0.7
QRPA	g_{pp} (max)[a] =144	0.2

[a]The authors of Ref. [65] use a δ interaction which has no *ab initio* microscopic background. The g_{pp} values are therefore different from those that appear in more recent QRPA calculations on the basis of more realistic NN potentials.

the various analyses and further indicates a high degree of similarity between the two (n, p)-type reactions.

In Ref. [36] the extracted GT strength was further compared to QRPA calculations by Engel *et al.* [65]. The calculations were performed using two extremes of the particle-particle interaction parameter g_{pp}. The two values of $g_{pp}(\mathrm{min}) = 130$ and $g_{pp}(\mathrm{max}) = 144$ were established by comparing calculated with experimental β^+-decay rates [65]. The resulting summed GT strength values for energies $E_x \leqslant 10$ MeV were $\Sigma B(\mathrm{GT}) = 0.7$ (lower limit of g_{pp}) and $\Sigma B(\mathrm{GT}) = 0.2$ (upper limit of g_{pp}).

IV. APPLICATION TO $2\nu\beta\beta$ DECAY

Because the $2\nu\beta\beta$-decay matrix element is a sum of products of two ordinary single GT matrix elements—one from the direction of β^+ and the other from β^-—according to

$$M_{\mathrm{DGT}}^{(2\nu)} = \sum_m \frac{\langle 0_{\mathrm{g.s.}}^{(f)} \| \sum_k \sigma_k \tau_k^- \| 1_m^+ \rangle \langle 1_m^+ \| \sum_k \sigma_k \tau_k^- \| 0_{\mathrm{g.s.}}^{(i)} \rangle}{{}^1\!/_2 Q_{\beta\beta}\left[0_{\mathrm{g.s.}}^{(f)}\right] + E_x(1_m^+) - E_0}$$
$$= \sum_m \frac{M_m(\mathrm{GT}^+) \cdot M_m(\mathrm{GT}^-)}{{}^1\!/_2 Q_{\beta\beta}\left[0_{\mathrm{g.s.}}^{(f)}\right] + E_x(1_m^+) - E_0}, \quad (4)$$

with

$$B_m(\mathrm{GT}^\pm) = \frac{1}{J_i + 1} \cdot |M_m(\mathrm{GT}^\pm)|^2, \quad (5)$$

we now examine the GT^- strength distribution obtained from the (p, n) experiment on ^{76}Ge performed by Madey *et al.* [37] at IUCF leading to the same intermediate nucleus ^{76}As. A comparison of the two spectral responses, i.e., the one through the $^{76}\mathrm{Ge}(p, n)$ reaction and the other through the $^{76}\mathrm{Se}(d, {}^2\mathrm{He})$ reaction, is shown in Fig. 5. We note that in the $(d, {}^2\mathrm{He})$ spectrum no isolated levels above $E_x = 2.5$ MeV can be identified above a general background response, while in the (p, n) spectrum 1^+ dominated structures were identified up to 3.5 MeV. An attempt was made to connect the levels in the two spectra by vertical lines, although we notice a slight energy-calibration mismatch between the two spectra. In

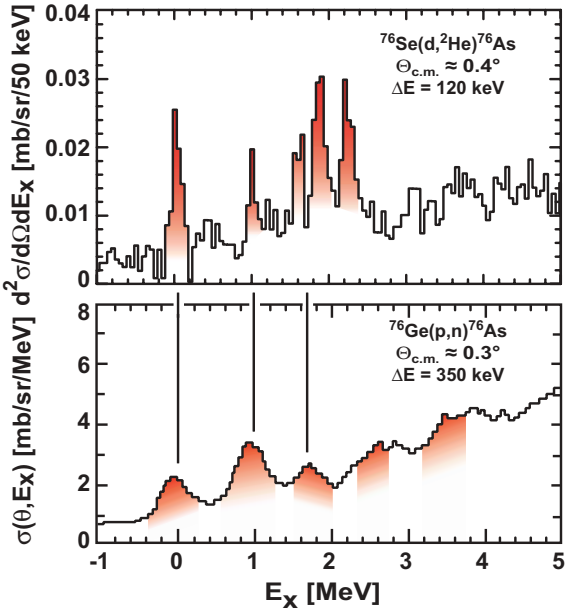

FIG. 5. (Color online) Excitation-energy spectra from the $^{76}\mathrm{Ge}(p, n)$ and $^{76}\mathrm{Se}(d, {}^2\mathrm{He})$ reactions populating the same levels in the intermediate nucleus ^{76}As. The shaded areas indicate predominant 1^+ transitions. The (p, n) spectrum was taken from Fig. 1 in Ref. [37].

Table III we present the extracted single- and double-β-decay matrix elements.

The final $2\nu\beta\beta$-decay matrix element is connected with the $2\nu\beta\beta$-decay rate via

$$\Gamma_{(\beta^-\beta^-)}^{2\nu} = G^{2\nu}(Q, Z)\left|M_{\mathrm{DGT}}^{(2\nu)}\right|^2, \quad (6)$$

with $G^{2\nu}(Q, Z)$ the phase-space factor depending on the weak-interaction coupling constant, the $Q_{\beta\beta}$ value of the decay, and the Z value of the decaying nucleus. With $Q_{\beta\beta} = 2.039$ MeV, the phase-space factor is calculated to be $G^{(2\nu)}\ln 2 = 1.3 \times 10^{-19}\,\mathrm{yr}^{-1}$ [33] in units of the electron

TABLE III. $B(\mathrm{GT})$ values and $M(\mathrm{GT})$ matrix elements extracted from the $^{76}\mathrm{Se}(d, {}^2\mathrm{He})$ and the $^{76}\mathrm{Ge}(p, n)$ charge-exchange reactions. Levels excited from both directions were used to determine an experimental $2\nu\beta\beta$ matrix element. The excitation energy is given in MeV and the matrix element in MeV^{-1}. Errors are indicated in parentheses and refer to the uncertainty in the last digits. The summed values have the statistical error as a superscript and the systematic error as a subscript. For the $B(\mathrm{GT}^-)$ values, the authors of Ref. [37] provide a statistical error of 3% and a systematic one of 13%.

E_x (MeV)	$B(\mathrm{GT}^+)$	$M(\mathrm{GT}^+)$	$B(\mathrm{GT}^-)$	$M(\mathrm{GT}^-)$	$M_{\mathrm{DGT}}^{(2\nu)}$ (MeV^{-1})
0.04/0.08	0.102(13)	0.32(2)	0.150(5)	0.387(6)	0.062(5)
0.5(3)	0.066(12)	0.26(2)	–	–	–
1.03	0.076(11)	0.28(2)	0.320(10)	0.566(8)	0.053(5)
1.63	0.077(11)	0.28(2)	–	–	–
1.86	0.141(16)	0.38(2)	0.180(5)	0.424(6)	0.044(3)
2.22	0.078(9)	0.28(2)	–	–	–
–	–	–	0.440(13)	0.663(10)	–
–	–	–	0.430(13)	0.656(10)	–
Σ	$0.54\,{}^{(3)}_{(8)}$	$1.79^{(5)}_{(13)}$	$1.52^{(2)}_{(20)}$	$2.70^{(2)}_{(18)}$	$0.159^{(7)}_{(22)}$

mass squared and with an unquenched axial-vector coupling constant g_A.

Assuming equal phases for each individual $2\nu\beta\beta$-decay matrix element in Eq. (4), one arrives at a total $2\nu\beta\beta$-decay matrix element of $M_{\mathrm{DGT}}^{(2\nu)} = (0.159 \pm 0.007(\mathrm{stat}) \pm 0.022\ (\mathrm{sys}))\ \mathrm{MeV}^{-1}$, from which the half-life of $T_{1/2}^{(2\nu)} = (1.17 \pm 0.11 \pm 0.33) \times 10^{21}$ yr can be evaluated and compared with the recommended average experimental value of $T_{1/2}^{(2\nu)} = (1.5 \pm 0.1) \times 10^{21}$ yr [21]. Given the coarse analysis due to the limited energy resolution of the (p, n) data (only three levels could be uniquely correlated, cf. Table III), the result is reassuring and seems to indicate that at least for the $2\nu\beta\beta$ decay the low-energy nuclear-structure part provides the leading contribution to the decay. Of course, phase cancellations among any of the individual matrix elements can change this picture dramatically. However, as GT^+ transitions are significantly Pauli-blocked for $N > Z$ nuclei ($N - Z = 8$ for ^{76}Se), one does not expect significant GT^+ strength at higher excitation energies, in accordance with what is observed. Clearly, high-resolution (^{3}He, t) measurements on ^{76}Ge would allow a much more detailed level-by-level comparison and thereby shed even more light on the size and the structure of the $2\nu\beta\beta$-decay matrix elements.

V. CONCLUSIONS

The present experimental study was aimed at contributing to the knowledge of nuclear matrix elements that are essential to the $2\nu\beta\beta$ decay but also have a role in the neutrinoless mode. The study focused on the mass-76 system, where the (n, p)-type ^{76}Se$(d, {}^2\mathrm{He})^{76}$As charge-exchange reaction at intermediate energies yielded GT^+ transitions to a number of individual low-lying levels. The GT^+ transitions define one of the two "legs" for the construction of the total nuclear matrix element that is active exclusively in the $2\nu\beta\beta$-decay mode and partially in the $0\nu\beta\beta$-decay mode. Although information about the second GT^- "leg" from earlier (p, n)-type charge-exchange reactions lacks the resolution, an attempt to combine both distributions yielded a half-life value for the $2\nu\beta\beta$ decay, which turned out to be in remarkably good agreement with the value known from the direct counting experiment. Special emphasis may be placed on the fact that the low-lying states (i.e., $E_x \lesssim 2$ MeV) seem to exhaust most of the strength needed to construct the full $2\nu\beta\beta$ matrix element. In fact, in the (n, p)-type direction no significant GT^+ strength could be detected at higher excitation energies, indicating that the higher excitation energy region may be of rather low importance at least for the 2ν-decay path.

ACKNOWLEDGMENTS

We thank H. Baumeister from the University of Münster for his dedication and perseverance in making outstanding targets. One of the authors, D.S., was supported by the DFG (SFB 634).

[1] W. P. Alford and K. P. Jackson (Eds.), *Proceedings of the Workshop on Isovector Excitations in Nuclei*, Can. J. Phys. **65**, (1987).
[2] C. D. Goodman *et al.*, Phys. Rev. Lett. **44**, 1755 (1980).
[3] T. N. Taddeucci *et al.*, Nucl. Phys. **A469**, 125 (1987).
[4] K. P. Jackson *et al.*, Phys. Lett. **B201**, 25 (1988).
[5] S. Rakers *et al.*, Phys. Rev. C **65**, 044323 (2002).
[6] E.-W. Grewe *et al.*, Phys. Rev. C **76**, 054307 (2007).
[7] E.-W. Grewe *et al.*, Phys. Rev. C **77**, 064303 (2008).
[8] GERDA Collaboration, LNGS P38/04 (2004).
[9] Majorana Collaboration, nucl-ex/0311013 (2003).
[10] V. Rodin, A. Faessler, F. Šimkovic, and P. Vogel, Nucl. Phys. **A766**, 107 (2006); **A793**, 213(E) (2007).
[11] O. Civitarese and J. Suhonen, Phys. Lett. **B626**, 80 (2005).
[12] R. Firestone and V. S. Shirley, *Table of Isotopes CD-rom*, 8th ed. (Wiley & Sons, 8-th Edition, New York, 1996).
[13] H. S. Miley, F. T. Avignone, R. L. Brodzinski, J. I. Collar, and J. H. Reeves, Phys. Rev. Lett. **65**, 3092 (1990).
[14] A. A. Vasenko *et al.*, Mod. Phys. Lett. A **5**, 1299 (1990).
[15] F. T. Avignone III *et al.*, Phys. Lett. **B256**, 559 (1991).
[16] C. E. Aalseth *et al.*, Nucl. Phys. **B48**, 223c (1996).
[17] M. Günther *et al.*, Phys. Rev. D **55**, 54 (1997).
[18] H. V. Klapdor-Kleingrothaus *et al.*, Eur. Phys. J. A **12**, 147 (2001).
[19] C. Dörr and H. V. Klapdor-Kleingrothaus, Nucl. Instrum. Methods Phys. Res. A **513**, 596 (2003).
[20] A. M. Bakalyarov *et al.*, Phys. Part. Nucl. Lett. **2**, 77 (2005).
[21] A. S. Barabash, Czech. J. Phys. **56**, 437 (2006).
[22] W. C. Haxton, in *Proceedings of the International Symposium on Nuclear Beta Decay and Neutrinos*, edited by T. Kotani, H. Ejiri and E. Takasugi (World Scientific, Singapore, 1986), p. 225.
[23] A. G. Williams and W. C. Haxton, AIP Conf. Proc. **176**, 924 (1988).
[24] M. Moe and P. Vogel, Annu. Rev. Nucl. Part. Sci. **44**, 247 (1994).
[25] A. A. Raduta, A. Escuderos, A. Faessler, E. Moya de Guerra, and P. Sarriguren, Phys. Rev. C **69**, 064321 (2004).
[26] K. Kaneko and M. Hasegawa, Prog. Theor. Phys. **105**, 219 (2001).
[27] E. Caurier, F. Nowacki, A. Poves, and J. Retamosa, Phys. Rev. Lett. **77**, 1954 (1996).
[28] V. A. Rodin, A. Faessler, F. Šimkovic, and P. Vogel, Phys. Rev. C **68**, 044302 (2003).
[29] M. Aunola and J. Suhonen, Nucl. Phys. **A602**, 133 (1996).
[30] A. Staudt, K. Muto, and H. V. Klapdor-Kleingrothaus, Europhys. Lett. **13**, 31 (1990).
[31] X. R. Wu *et al.*, Phys. Lett. **B272**, 169 (1991); **B276**, 274 (1992).
[32] M. Honma, T. Otsuka, T. Mizusaki, and M. Hjorth-Jensen, J. Phys. Conf. Ser. **49**, 45 (2006).
[33] J. Suhonen and O. Civitarese, Phys. Rep. **300**, 123 (1998).
[34] J. Suhonen, Phys. Lett. **B607**, 87 (2005).
[35] A. Faessler *et al.*, arXiv:nucl-th/0711.3996v2 (2008).
[36] R. L. Helmer *et al.*, Phys. Rev. C **55**, 2802 (1997).
[37] R. Madey *et al.*, Phys. Rev. C **40**, 540 (1989).
[38] C. D. Goodman *et al.*, IEEE Trans. Nucl. Sci. **26**, 2248 (1979).
[39] R. L. Helmer, Can. J. Phys. **65**, 588 (1987).

[40] A. M. van den Berg, Nucl. Instrum. Methods Phys. Res. B **99**, 637 (1995).
[41] H. J. Wörtche, Nucl. Phys. **A687**, 321c (2001).
[42] M. Hagemann *et al*., Nucl. Instrum. Methods Phys. Res. A **437**, 459 (1999).
[43] B. A. M. Krüsemann *et al*., IEEE Trans. Nucl. Sci. **47**, 2741 (2000).
[44] V. M. Hannen *et al*., Nucl. Instrum. Methods Phys. Res. A **500**, 68 (2003).
[45] C. Bäumer *et al*., Phys. Rev. C **71**, 024603 (2005).
[46] C. Bäumer *et al*., Phys. Rev. C **68**, 031303(R) (2003).
[47] E.-W. Grewe *et al*., Phys. Rev. C **69**, 064325 (2004).
[48] S. Rakers *et al*., Phys. Rev. C **70**, 054302 (2004).
[49] C. Bäumer *et al*., Phys. Rev. C **71**, 044003 (2005).
[50] S. Rakers *et al*., Nucl. Instrum. Methods Phys. Res. A **481**, 253 (2002).
[51] S. Rakers *et al*., Phys. Rev. C **71**, 054313 (2005).
[52] L. Popescu *et al*., Phys. Rev. C **75**, 054312 (2007).
[53] A. Negret *et al*., Phys. Rev. Lett. **97**, 062502 (2006).
[54] H. Okamura, Phys. Rev. C **60**, 064602 (1999).
[55] A. Korff *et al*., Phys. Rev. C **70**, 067601 (2004).
[56] A. J. Koning and J. P. Delaroche, Nucl. Phys. **A713**, 231 (2003).
[57] M. A. Franey and W. G. Love, Phys. Rev. C **31**, 488 (1985).
[58] A. Bohr and B. R. Mottelson, *Nuclear Structure* (Benjamin, New York, 1975), Vols. 1 and 2.
[59] M. A. Hofstee *et al*., Nucl. Phys. **A588**, 729 (1995); S. Y. van der Werf, computer code NORMOD, KVI Groningen, 1991 (unpublished).
[60] R. G. T. Zegers *et al*., Phys. Rev. C **74**, 024309 (2006).
[61] A. L. Cole *et al*., Phys. Rev. C **74**, 034333 (2006).
[62] Y. Fujita *et al*., Phys. Rev. C **75**, 057305 (2007).
[63] R. G. T. Zegers *et al*., Phys. Rev. C **77**, 024307 (2008).
[64] W. G. Love and M. A. Franey, Phys. Rev. C **24**, 1073 (1981).
[65] J. Engel, P. Vogel, and M. R. Zirnbauer, Phys. Rev. C **37**, 731 (1988).
[66] M. C. Vetterli *et al*., Phys. Rev. C **45**, 997 (1992).